Artificial Neural Network Modeling of Solubilities of 21 Commonly Used Industrial Solid Compounds in Supercritical Carbon Dioxide

ARTICLE *in* INDUSTRIAL & ENGINEERING CHEMISTRY RESEARCH · NOVEMBER 2010

Impact Factor: 2.59 · DOI: 10.1021/ie101545g · Source: OAI

4 AUTHORS:

Farhad Gharagheizi
Texas Tech University
168 PUBLICATIONS **2,911** CITATIONS
SEE PROFILE

Ali Eslamimanesh
OLI Systems
106 PUBLICATIONS **1,754** CITATIONS
SEE PROFILE

Amir H. Mohammadi
558 PUBLICATIONS **4,819** CITATIONS
SEE PROFILE

Dominique Richon
Aalto University
533 PUBLICATIONS **6,595** CITATIONS
SEE PROFILE

Artificial Neural Network Modeling of Solubilities of 21 Commonly Used Industrial Solid Compounds in Supercritical Carbon Dioxide

Farhad Gharagheizi,[†,‡] Ali Eslamimanesh,[§] Amir H. Mohammadi,[*,§,||] and Dominique Richon[§]

Department of Chemical Engineering, Faculty of Engineering, University of Tehran, P.O. Box 11365-4563, Tehran, Iran, MINES ParisTech, CEP/TEP - Centre Énergétique et Procédés, 35 Rue Saint Honoré, 77305 Fontainebleau, France, and Thermodynamics Research Unit, School of Chemical Engineering, University of KwaZulu-Natal, Howard College Campus, King George V Avenue, Durban 4041, South Africa

In this communication, a feed-forward artificial neural network algorithm has been applied to calculate/predict the solubilities of 21 of the commonly used industrial solid compounds in supercritical carbon dioxide. An optimized three-layer feed-forward neural network using critical properties of solute and operating temperature and pressure is presented. Application of the model for 795 data points of 21 compounds gives a squared correlation coefficient of 0.9533 and an average absolute deviation of about 14% from the experimental values.

1. Introduction

Applications of supercritical fluids (SCFs) in the chemical industries have been of much interest in recent years. They have been widely used in extractions, purifications, separations, crystal growth, reactions, and fractionations.[1,2] Carbon dioxide, being inexpensive, nonexplosive, readily available, and easily separated from the extracted products,[1,3] is considered to be the most suitable fluid in supercritical processes, for example, for the extraction of fatty acid esters, vegetable oils, and antioxidants in the food engineering industry and for dissolving solid phenazopyridine, propranolol, and methyl salicylate in the pharmaceutical industry.[4,5]

To design optimized supercritical processes, solubility data of the considered compounds are needed. There are different thermodynamic approaches for representing these data.[6] A preliminary study shows that the available models fall into three main categories: equations of state, empirical models, and cluster solvation models.

In the first group, different equations of state (EoS) along with various mixing rules are used. Kurnik and Reid,[7] Kosal and Holder,[8] Goldman et al.,[9] Cortesi et al.,[10] and Goodarznia and Esmaielzadeh[11] are among the researchers who have developed thermodynamic models based on cubic equations of state such as the Redlich−Kwong (RK),[12] Soave−Redlich−Kwong (SRK),[13] and Peng−Robinson (PR)[14] EoS with conventional mixing rules. However, the mixing rules are sometimes accompanied by excess Gibbs energy (G^{ex}) models, especially because the performance of traditional two-parameter equations of state may be doubtful in the supercritical fluid region. The Patel−Teja (PT) EoS[15] was first used by Sheng et al.[16] with modified Huron−Vidal[17] mixing rules to represent/estimate the solubilities of aromatic compounds in supercritical carbon dioxide. Later, Huang et al.[2] applied mixing rules with the UNIFAC activity coefficient model to calculate the solid solubilities of aromatic, fatty acid, and heavy alcohol compounds in supercritical CO_2. Their proposed model led to reliable results for both polar and nonpolar compounds. In 1997, Zhong and Masuoka[18] developed a new UNIFAC G^{ex}/EoS thermodynamic model using perturbed hard-sphere (PHS) theory.[18] This technique was also applied by Esmaeilzadeh and co-workers[1] to derive a new mixing rule based on the nonrandom two-liquid (NRTL) model[1] for the SRK[13] and PR[14] equations of state. Their model was successful in predicting the solubilities of hydrocarbons, aliphatic carboxylic acids, aromatic acids, and aromatic alcohols in supercritical carbon dioxide. In addition, a novel lattice EoS developed by Kumar[19] has been applied successfully for triglyceride solubility calculations.[20]

Another recent attempt was made by Martinez-Correa et al.[21] to calculate the solubility of squalene in supercritical carbon dioxide using the group contribution equation of state (GC-EoS). Tsivintzelis et al.[22] also predicted the phase behavior of mixtures of pharmaceuticals with liquid or supercritical solvents applying the nonrandom hydrogen-bonding (NRHB) theory and obtained reliable predictions. Descriptions of other EoS-based models can be found elsewhere.[23−28]

Several groups have studied the possibility of using empirical equations for phase equilibria calculations of mixtures of supercritical carbon dioxide and solid substances. Chrastil[29] related the solubility of a solute to the density of the supercritical solvent with the assumption that the molecule of a solute associates with a certain number of molecules of gas with the formation of a solvate complex that is in equilibrium with the gas.[30] This semiempirical model, which contains three adjustable parameters to minimize the deviation of the calculated solubility values from experimental values, was used by Knez et al.[30] to accurately calculate the solubilities of ametryn, prometryn, atrazine, and simazine in supercritical CO_2. An alternative method was proposed by Mendez-Santiago and Teja,[31] who applied a semiempirical equation including three parameters for each binary system.[2] These methods have been extended by other authors to model the behavior of different solid compound + supercritical CO_2 mixtures.[32,33]

The third class of models investigates the clusterlike behavior of a solute in the supercritical phase. Zhong et al.[34] and Jiang et al.[35] developed such models by correlating the solubilities of solid materials in supercritical fluid. Using temperature-

* To whom correspondence should be addressed. E-mail: amir-hossein.mohammadi@ensmp.fr. Tel.: + (33) 1 64 69 49 65. Fax: + (33) 1 64 69 49 68.

[†] University of Tehran.

[‡] Current address: Saman Energy Giti Co., Tehran, Iran, Postal Code: 3331619636.

[§] MINES ParisTech.

[||] University of KwaZulu-Natal.

10.1021/ie101545g

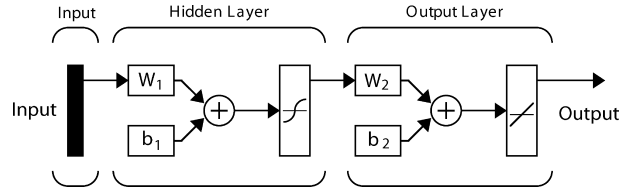

Figure 1. Schematic structure of a 3FFNN, such as that used in this study.

dependent parameters, they reported satisfactory results on binary systems, but no attempt was made to extend the model to multicomponent mixtures until 2003, when Cheng and co-workers[6] presented a simplified cluster solvation method to do so. They also compared the obtained results with previous models from all three categories described before.

Even though all of the proposed models are successful in calculations/predictions for many kinds of solid compounds in supercritical carbon dioxide, they have some shortcomings. For example, for several approaches, the large observed deviations of the results from experimental data cause users to doubt the reliability of the predictions. Therefore, in light of the ever-growing application of SCF industrial processes, there is a strong need to identify general and reliable techniques that can predict the solubilities of solid compounds in supercritical carbon dioxide. In this work, we have focused on the use of an artificial neural network (ANN) for this purpose.

2. Artificial Neural Network Algorithm

Artificial neural networks are composed of simple elements working in a parallel computational strategy. These elements are inspired by biological nervous systems[36−40] and are called neurons.

So far, several types of ANN strategies have been proposed.[36] One of the most widely used is called the three-layer feed-forward neural network (3FFNN) with sigmoid (hyperbolic) transfer function. This type of ANN is used to generate a nonlinear correlation between input and output parameters. In other words, this strategy is somehow used as a regression tool. The schematic structure of a 3FFNN is shown in Figure 1. This type of ANN contains three layers. The first one is the input layer. The second is the hidden layer of the 3FFNN, which consists of n neurons. The parameter n is one of the main parameters of the 3FFNN method and should be obtained by postoptimization after the base structure of the 3FFNN has been generated. The mathematical formulation of this strategy can be written as

$$\text{output}(i) = W_2 \tanh[W_1 \text{input}(i) + b_1] + b_2 \qquad (1)$$

where i refers to the data point, the parameter W_1 is the weight relating the first layer to the second layer, W_2 is the weight relating the second layer to the third (or output) layer, b_1 denotes the bias to the second layer, and b_2 stands for the bias of the third (output) layer. W_1, W_2, b_1, and b_2 should be determined by a process called training.

Generally, in many scientific and engineering problems, input and output parameters should be defined for solving the problem. To generate a 3FFNN model, there is a need to know some parameters of the proposed problem. The required parameters are the number of inputs (n_{ip}); the number of outputs (n_{op}); and the number of objects (n_{obj}), that is, the number of data points with known input parameter (ip) and corresponding output parameter (op). For instance, in a problem with six input parameters and one output parameter with 795 data points, the values of n_{ip}, n_{op}, and n_{obj} are 6, 1, and 795, respectively.

Table 1. Physical Properties of the Compounds Used in This Work

component	T_c (K)	P_c (MPa)	ω	v^s (cm^3/mol)	ref[a]
carbon dioxide	304.2	7.383	0.224	−	61
triphenylene	1013.6	2.928	0.492	175	6
phenazopyridine	1148.4	2.756	0.735	160.3	64
propranolol	958.5	2.2	1.061	214.3	64
methyl salycilate	700	4.07	0.631	130	GCM[a]
fluoranthene	905	2.61	0.587	161.55	GCM
naphthalene	748.35	4.051	0.302	112.43	1
cholesterol	959	1.25	0.95	367.54	GCM
benzocaine	699.4	4.22	0.36	141.87	GCM
benzoin	853.52	2.66	0.599	162	1
aspirin	762.9	3.28	0.817	128.68	GCM
acenaphthene	803.15	31	0.38	126.19	GCM
perylene	863	8.68	0.915	201.85	GCM
mandelic acid	903.79	34.73	0.645	117	1
propyl 4-hydroxybenzoate	815.92	31.3	0.722	131.6	1
lactic acid	627	59.6	1.029	75	GCM
stearic acid	779	13.4	1.084	302.4	1
1-eicosanol	792	12.2	0.937	355.2	6
phenol	692.2	60.5	0.45	89	6
p-chlorophenol	724.75	53.61	0.456	101.4	GCM
2,4-dichlorophenol	718.38	53.04	0.608	117.9	GCM
2,4,6-trichlorophenol	745.96	51.52	0.522	132.6	GCM
methimazole	731.7	60.75	0.442	162.1	3

[a] GCM: Properties evaluated by group contribution method proposed in refs 59 and 60.

One can determine the dimensions of each part in eq 1 using n neurons. The input (i) is a row containing n_{ip} input parameters of the ith object, so it is of dimensions $n_{ip} \times 1$, and W_1 is of dimensions $n \times n_{ip}$. Therefore, $W_1 \times$ input(i) should be of dimensions $n \times n_{ip}$. b_1 is of dimensions $n \times n_{ip}$. Thus, the results of the second layer output are of dimensions $n \times 1$. It is easy to figure out the dimensions of W_2 and B_2: W_2 should be of dimensions $n_{op} \times n$, and b_2 should be of dimensions $n_{op} \times 1$. As a result, output(i) is of dimensions $n_{op} \times 1$.

The unknown parameters for a desired number of neurons n in a 3FFNN model are W_1, W_2, b_1, and b_2. These parameters should be obtained using the training process, as mentioned earlier. This process applies an optimization method to minimize an objective function defined between the output and available experimental values. One of the most widely used objective functions employed in the 3FFNN training process is the mean square of errors (MSE).

The parameters W_1, W_2, b_1, and b_2 are the most significant factors for selecting an optimization method. First and perhaps most importantly, the method should be accurate enough to deal with the specified problem. Another element to consider is that the applied method should be robust when there are several tens or hundreds of parameters in a simple 3FFNN. In this work the Levenberg−Marquardt (LM) optimization algorithm[36] is used because previous studies have shown that it is one of the most appropriate methods in terms of the mentioned characteristics.[41−57]

Some empirical correlations[58] are available for determining the value of n (the number of neurons in the hidden layer) of a 3FFNN; however, it completely depends on the nature of the problem. Therefore, it should be postoptimized; that is, searching must be done to find the best value of n.

Of particular interest is the fact that the data set should be divided into three data subsets. This process is needed to ensure the validity of the obtained 3FFNN, as well as to show its prediction capability. It is required that the main data set be divided into three subsets called the training set, the validation set, and the test set. In this work, these sets are defined as follows: The test set is used to generate the 3FFNN model. The validation set is applied to control the optimization process of training. The test set is used to test the prediction capability of

Table 2. Statistical Parameters of the Presented Model

statistical parameter	value
Training Set	
$R^{2\,c}$	0.9540
average absolute deviation[a]	13.2%
standard deviation error	0.020
root-mean-square error	0.004
N^b	717
Validation Set	
R^2	0.9306
average absolute deviation	16.5%
standard deviation error	0.019
root-mean-square error	0.006
N	39
Test Set	
R^2	0.9721
average absolute deviation	19.7%
standard deviation error	0.020
root-mean-square error	0.003
N	39
Training Set + Validation Set + Test Set	
R^2	0.9533
average absolute deviation	14.2%
standard deviation error	0.020
root-mean-square error	0.004
N	795

[a] AAD (%) = $(100/N)\sum_i^N$|[calculated(i)/predicted(i) − experimental(i)]|/[experimental(i)]. [b] Number of data points. [c] R^2: squared correlation coefficient.

the obtained 3FFNN. The effect of the allocation percentage of each of the three subsets from the main data set was studied previously.[58]

3. Investigated Compounds

Supercritical processes deal with many chemical compounds. Twenty-one typical compounds are investigated in this study to present a comprehensive reliable regression. The physical properties of the compounds are needed to begin the calculations. Table 1 lists these values along with references. A group contribution method[59,60] was applied to evaluate the required properties when not experimentally available.

4. Results and Discussion

In the first step, the input and output parameters of the model are defined. The input parameters include the critical temperature (T_c); the critical pressure (P_c); the acentric factor (ω); and the molar volume of each investigated solute (v^s) at the desired temperature and pressure, along with the temperature (T) and pressure (P). Therefore, n_{ip} is equal to 6.

The possibility of mapping the data onto a smoother space should be paid much attention in the calculations. Generally, the solubilities of solid compounds in supercritical carbon dioxide range from 3×10^{-7} to 1.11×10^{-1}.[64−76] Therefore, the natural logarithm of solubility was regarded as the output of the 3FFNN algorithm to decrease computational errors. This was done to prevent the possibility of obtaining negative output values (trivial values) for the solubility. Furthermore, the natural logarithm is a useful function to map a data set that spans several orders of magnitude onto a smoother space. Considering this mathematical issue, the solubility space was transferred to a new space that ranges from −15 to −2.2. Thus, n_{op} is equal to 1.

In the next step, the main data set was divided into three subsets. The training set comprised 90% of the main data set, that is, 717 data points. The validation and test sets each contained 5% of the main data set. In other words, each one contained 39 data points. Consequently, n_{obj} is 717. The process of division of the available data into the subsets was random.

Finally, several 3FFNNs modules were generated assuming values of 1−50 for n (number of neurons in the hidden layer) using the previously described procedure. The most accurate results were observed at $n = 20$. It should be noted that this value of n is not the global value, because the optimization method used to train the ANN has significant effects on the

Table 3. Solubility Values Calculated by the Presented Model along with Absolute Average Deviations from Experimental Data[4,5,64−76]

compound	temperature range (K)	pressure range (MPa)	N^a	calculated/predicted solubility range		AAD[b] (%)	ref[c]
triphenylene	308.15−328.15	8.5−25.1	27	$[3.48 \times 10^{-6}$	$3.35 \times 10^{-5}]$	8	64
phenazopyridine	308−348	12.2−35.5	45	$[5.19 \times 10^{-5}$	$1.19 \times 10^{-4}]$	8	4
propranolol	308−348	12.2−35.5	83	$[1.34 \times 10^{-5}$	$2.40 \times 10^{-3}]$	9.8	4
methyl salycilate	343.15−423.15	9.0−31.0	44	$[7.20 \times 10^{-4}$	$8.16 \times 10^{-2}]$	13.56	5
fluoranthene	308.15−328.15	8.6−24.9	28	$[9.20 \times 10^{-6}$	$6.75 \times 10^{-4}]$	10.29	64
naphthalene	308.15−33.35	8.2−29.1	51	$[1.47 \times 10^{-5}$	$7.15 \times 10^{-2}]$	11.62	65
cholestrol	313.1−333.1	10.0−25.0	17	$[2.54 \times 10^{-6}$	$1.41 \times 10^{-4}]$	7.64	66
benzocain	308−348	8.4−35.5	52	$[2.95 \times 10^{-5}$	$1.28 \times 10^{-2}]$	33.16	67, 68
benzoin	308.15−328.15	11.13−24.43	19	$[3.33 \times 10^{-5}$	$4.62 \times 10^{-4}]$	10.87	69
aspirin	308.15−328.15	12.0−25.0	24	$[6.51 \times 10^{-5}$	$3.41 \times 10^{-4}]$	9.15	70
acenaphthene	308.15−348.15	12.16−35.46	45	$[1.32 \times 10^{-3}$	$1.52 \times 10^{-2}]$	11.95	71
perylene	313−523	10.0−45.0	30	$[3.35 \times 10^{-7}$	$7.11 \times 10^{-4}]$	10.84	72
mandelic acid	308.15−328.15	10.1−23.06	21	$[2.44 \times 10^{-5}$	$2.74 \times 10^{-3}]$	8.92	69
propyl 4-hydroxybenzoate	308.15−328.15	9.41−22.09	21	$[2.05 \times 10^{-5}$	$4.43 \times 10^{-4}]$	9.84	69
lactic acid	313−328	5.82−19.71	29	$[2.03 \times 10^{-5}$	$1.52 \times 10^{-3}]$	12.98	73
stearic acid	318−338	14.54−46.75	17	$[4.52 \times 10^{-4}$	$1.42 \times 10^{-2}]$	22.67	74
1-eicosanol	308.2−328.2	3.62−41.23	24	$[1.47 \times 10^{-5}$	$2.07 \times 10^{-4}]$	13.55	76
phenol	309.2−363.15	8.0−35.0	77	$[7.40 \times 10^{-4}$	$8.87 \times 10^{-2}]$	13.69	61, 75
p-chlorophenol	309.2−333.2	8.0−19.84	36	$[9.97 \times 10^{-4}$	$4.14 \times 10^{-2}]$	8.59	61
2,4-dichlorophenol	309.2−318.2	7.01−19.84	30	$[7.99 \times 10^{-4}$	$1.11 \times 10^{-1}]$	22.81	61
2,4,6-trichlorophenol	309.2−333.2	7.85−19.61	75	$[3.33 \times 10^{-4}$	$8.59 \times 10^{-2}]$	23.61	61
total			795			14.2	
				predicted solubility range			
methimazole	308−348	12.2−35.5	40	$[4.478 \times 10^{-6}$	$1.956 \times 10^{-4}]$	8.9	4

[a] Number of experimental data points. [b] AAD (%) = $(100/N)\sum_i^N$|[calculated(i)/predicted(i) − experimental(i)]|/[experimental(i)]. [c] References of experimental data.

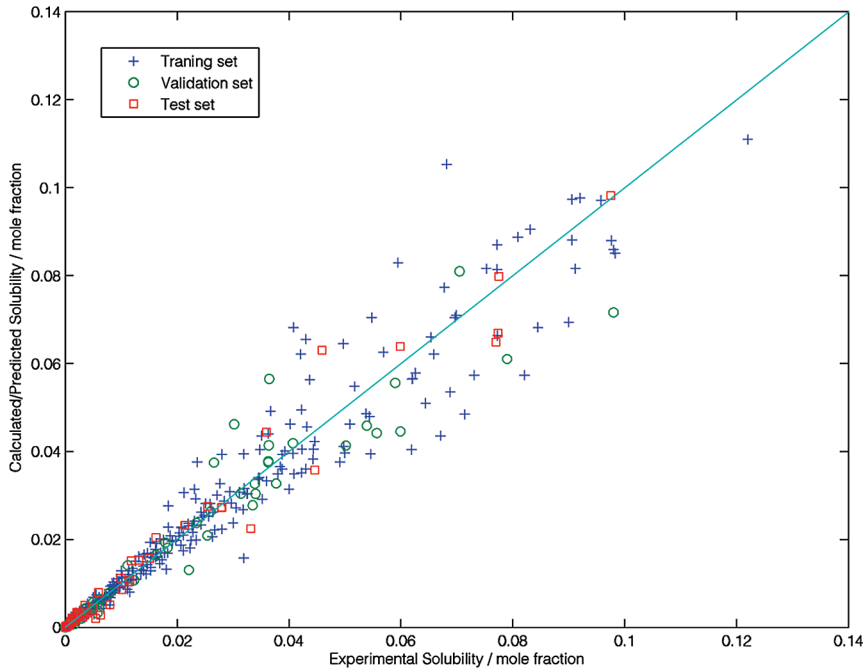

Figure 2. Experimental data[4,5,64−76] versus the presented model-calculated/-predicted solubility results (mole fraction).

obtained value. As previously stated, the Levenberg−Marquardt algorithm[36] was used to train the ANN module.[41−57] More accurate optimization methods other than this algorithm are available; however, they require much longer convergence times. In other words, the more accurate the optimization method, the more time needed for the algorithm to converge to the global optimum. The LM is the most widely used algorithm for training because it is robust and accurate enough to deal with the considered systems.[41−57]

The statistical parameters of the model are listed in Table 2. Table 3 reports the values of the solubilities calculated by the presented ANN model. The comparison between the calculated and experimental values is depicted in Figure 2 for the three subsets used in this study. To further check the prediction capability of the presented model, the solubility in supercritical carbon dioxide of methimazole (which was not used in the development of the algorithm) was predicted. As can be seen in Table 3, the predicted results coincide well with the existing experimental values.

The squared correlation coefficients (R^2), average absolute deviations, standard deviation errors, and root-mean-square errors of the model over the training set, validation set, test set, and main data set were calculated as 0.9540, 0.9306, 0.9720, and 0.9533; 13.2%, 16.5%, 19.7%, and 14.2%; 0.020, 0.019, 0.020, and 0.020; and 0.004, 0.006, 0.003, and 0.004, respectively.

The mat file (MATLAB software file) of the obtained 3FFNN model is available free of charge upon request from the authors. Furthermore, the procedure of application of the program is presented in the Appendix.

5. Conclusions

In this work, a three-layer feed-forward neural network was successfully applied for calculation/prediction of the solubilities of 21 solid substances in supercritical carbon dioxide. The critical temperature; critical pressure; acentric factor; and molar volume of each solute at a specific temperature and pressure, along with that temperature and pressure, were treated as input parameters. The results demonstrate that the model is capable of estimating the solubility of the investigated solid compounds in supercritical carbon dioxide with an average absolute deviation of about 14% from the experimental values.

Acknowledgment

A.E. thanks MINES ParisTech for providing a Ph.D. scholarship.

Appendix

The model is easy to apply. What is needed is to just drag and drop the mat file into a MATLAB environment (any versions) workspace. Let us get a response from the model step by step:

First, assume that we want to see the model response for the solubility of triphenylene in supercritical carbon dioxide at a temperature of 308.15 K and a pressure of 103 bar. The critical temperature, critical pressure, acentric factor, and molar density of triphenylene are equal to 1013.6 K, 29.28 bar, 0.492, and 175 cm^3/mol, respectively. After drag and drop the mat file, do as follows in the MATLAB workspace:

```
Triphenylene_i=[ 1013.6
                 29.28
                 0.492
                 175
                 308.15
                 103];
Triphenylene_o=sim(results.net, Triphenylene_i);
Triphenylene_s=exp(Triphenylene_o )
```

Therefore, one will observe the estimated solubility as follows: 9.3556e-006.

The experimental value for this solubility is equal to 8.38×10^{-6}. Therefore, the absolute relative deviation of the calculated value from the experimental one is 11.7%.

Supporting Information Available: Solubilities calculated/predicted by the presented ANN model along with absolute

deviations of the results from the experimental values and different types of data subsets. This material is available free of charge via the Internet at http://pubs.acs.org.

Literature Cited

(1) Esmaeilzadeh, C. F.; As'adi, C. H.; Lashkarbolooki, M. Calculation of the solid solubilities in supercritical carbon dioxide using a new G^{ex} mixing rule. *J. Supercrit. Fluids* **2009**, *51*, 148–158.

(2) Huang, C.; Tang, M.; Tao, W.; Chen, Y. Calculation of the solid solubilities in supercritical carbon dioxide using a modified mixing model. *Fluid Phase Equilib.* **2001**, *179*, 67–84.

(3) Housaindokht, M. R.; Haghighi, B.; Bozorgmehr, M. R. A comparison among three equations of state in predicting the solubility of some solids in supercritical carbon dioxide. *Korean J. Chem. Eng.* **2007**, *24/1*, 102–105.

(4) Yamini, Y.; Arab, J.; Asghari-khiavi, M. Solubilities of phenazopyridine, propranolol, and methimazole in supercritical carbon dioxide. *J. Pharm. Biomed. Anal.* **2003**, *32*, 181–187.

(5) Ismadji, S. Solubility of methyl salicylate in supercritical carbon dioxide at several temperatures. *J. Chem. Eng. Data* **2008**, *53*, 2207–2210.

(6) Cheng, K.; Tang, M.; Chen, Y. Calculations of solid solubility in supercritical fluids using a simplified cluster solvation model. *Fluid Phase Equilib.* **2003**, *214*, 169–186.

(7) Kurnik, R. T.; Reid, R. C. Solubility of solid mixtures in supercritical fluids. *Fluid Phase Equilib.* **1982**, *8*, 93–105.

(8) Kosal, E.; Holder, G. D. Solubility of anthracene and phenanthrene mixtures in supercritical carbon dioxide. *J. Chem. Eng. Data* **1987**, *32*, 148–150.

(9) Goldman, S.; Gray, S. G.; Li, W.; Tomberli, B.; Joslin, C. G. Predicting solubilities in supercritical fluids. *J. Phys. Chem.* **1996**, *100*, 7246–7249.

(10) Cortesi, A.; Kikic, I.; Alessi, P.; Turtoi, G.; Garnier, S. Effect of chemical structure on the solubility of antioxidants in supercritical carbon dioxide: Experimental data and correlation. *J. Supercrit. Fluids* **1999**, *14*, 139–144.

(11) Goodarznia, I.; Esmaeilzadeh, F. Solubility of an anthracene, phenanthrene, and carbazole mixture in supercritical carbon dioxide. *J. Chem. Eng. Data* **2002**, *47*, 333–338.

(12) Redlich, O.; Kwong, J. N. S. On the thermodynamics of solutions. V. An equation of state. Fugacities of gaseous solutions. *Chem. Rev.* **1949**, *44*, 233–244.

(13) Soave, G. Equilibrium constants for modified Redlich−Kwong equation of state. *Chem. Eng. Sci.* **1972**, *27*, 1197–1203.

(14) Peng, D. Y.; Robinson, D. B. A new two-constant equation of state. *Ind. Eng. Chem. Fundam.* **1976**, *15*, 59–64.

(15) Patel, N. C.; Teja, A. C. A new cubic equation of state for fluids and fluid mixtures. *Chem. Eng. Sci.* **1982**, *37*, 463–473.

(16) Sheng, Y. J.; Chen, P. C.; Chen, Y. P.; Wong, D. S. H. Calculations of solubilities of aromatic compounds in supercritical carbon dioxide. *Ind. Eng. Chem. Res.* **1992**, *31*, 967–973.

(17) Michelsen, M. L. A modified Huron−Vidal mixing rule for cubic equations of state. *Fluid Phase Equilib.* **1990**, *60*, 213–219.

(18) Zhong, C.; Masuoka, H. An EOS/G^E type mixing rule for perturbed hard-sphere equation of state and its application to the calculation of solid solubility in supercritical carbon dioxide. *Fluid Phase Equilib.* **1997**, *141*, 13–23.

(19) Kumar, S. Environmental problems: Fundamental studies and global ramifications. Sc.D. Thesis, Massachusetts Institute of Technology, Cambridge, MA, 1986.

(20) Bamberger, T.; Erickson, J. C.; Cooney, C. L.; Kumar, S. K. Measurement and model prediction of solubilities of pure fatty acids, pure triglycerides, and mixtures of triglycerides in supercritical carbon dioxide. *J. Chem. Eng. Data* **2008**, *53*, 2207–2210.

(21) Martinez-Correa, H. A.; Gomes, D. C. A.; Kanehisa, S. L.; Cabral, F. A. Measurements and thermodynamic modeling of the solubility of squalene in supercritical carbon dioxide. *J. Food Eng.* **2010**, *96*, 43–50.

(22) Tsivintzelis, I.; Economou, I. G.; Kontogeorgis, G. Modeling the phase behavior in mixtures of pharmaceuticals with liquid or supercritical solvents. *J. Phys. Chem. B* **2009**, *113*, 6446–6458.

(23) Johnston, K. P.; Peck, D. G.; Kim, S. Modeling supercritical mixtures: How predictive is it. *Ind. Eng. Chem. Res.* **1989**, *28*, 1115–1125.

(24) Brennecke, J. F.; Eckert, C. A. Phase equilibria for supercritical fluid process design. *AIChE J.* **1989**, *35*, 1409–1427.

(25) Mukhopadhyay, M.; Rao, G. V. R. Thermodynamic modeling for supercritical fluid process design. *Ind. Eng. Chem. Res.* **1993**, *32*, 922–930.

(26) Song, W. Y.; Sadus, R. J. Equations of state for the calculation of fluid-phase equilibria. *AIChE J.* **2000**, *46*, 169–196.

(27) Madras, G. Thermodynamic modeling of the solubilities of fatty acids in supercritical fluids. *Fluid Phase Equilib.* **2004**, *220*, 167–169.

(28) Khimeche, K.; Alessi, P.; Kikic, I.; Dahmanib, A. Solubility of diamines in supercritical carbon dioxide: Experimental determination and correlation. *J. Supercrit. Fluids* **2007**, *41*, 10–19.

(29) Chrastil, J. Solubility of solids and liquids in supercritical gases. *J. Phys. Chem.* **1982**, *86*, 3016–3021.

(30) Knez, Z.; Rizňer-Hraša, A.; Kokota, K.; Bauman, D. Solubility of some solid triazine herbicides in supercritical carbon dioxide. *Fluid Phase Equilib.* **1998**, *152*, 95–108.

(31) Mendez-Santiago, J.; Teja, A. S. The solubility of solids in supercritical fluids. *Fluid Phase Equilib.* **1999**, *158−160*, 501–510.

(32) Mendez-Santiago, J.; Teja, A. S. Solubility of solids in supercritical fluids: Consistency of data and a new model for cosolvent systems. *Ind. Eng. Chem. Res.* **2000**, *39*, 4767–4771.

(33) Liong, K. K.; Foster, N. R.; Ting, S. S. T. Solubility of fatty acid esters in supercritical carbon dioxide. *Ind. Eng. Chem. Res.* **1992**, *31*, 400–404.

(34) Zhong, M.; Han, B.; Ke, J.; Yan, H.; Peng, D. Y. A model for correlating the solubility of solids in supercritical CO_2. *Fluid Phase Equilib.* **1998**, *146*, 93–102.

(35) Jiang, C.; Pan, Q.; Pan, Z. Solubility behavior of solids and liquids in compressed gases. *J. Supercrit. Fluids* **1998**, *12*, 1–9.

(36) Hagan, M.; Demuth, H. B.; Beale, M. H. *Neural Network Design*; International Thomson Publishing: Singapore, 2002.

(37) Chouai, A.; Laugier, S.; Richon, D. Modeling of thermodynamic properties using neural networks: Application to refrigerants. *Fluid Phase Equilib.* **2002**, *199*, 53–62.

(38) Piazza, L.; Scalabrin, G.; Marchi, P.; Richon, D. Enhancement of the extended corresponding states techniques for thermodynamic modelling. I. Pure fluids. *Int. J. Refrig.* **2006**, *29*, 1182–1194.

(39) Scalabrin, G.; Marchi, P.; Bettio, L.; Richon, D. Enhancement of the extended corresponding states techniques for thermodynamic modelling. II. Mixtures. *Int. J. Refrig.* **2006**, *29*, 1195–1207.

(40) Chapoy, A.; Mohammadi, A. H.; Richon, D. Predicting the hydrate stability zones of natural gases using Artificial Neural Networks. *Oil Gas Sci. Technol.: Rev. IFP* **2007**, *62*, 701–706.

(41) Gharagheizi, F. A new group contribution-based method for estimation of lower flammability limit of pure compounds. *J. Hazard. Mater.* **2009**, *170*, 595–604.

(42) Gharagheizi, F. New neural network group contribution model for estimation of lower flammability limit temperature of pure compounds. *Ind. Eng. Chem. Res.* **2009**, *48*, 7406–7416.

(43) Gharagheizi, F.; Sattari, M. Estimation of molecular diffusivity of pure chemicals in water: a quantitative structure−property relationship study. *SAR QSAR Environ. Res.* **2009**, *20*, 267–285.

(44) Gharagheizi, F. Prediction of standard enthalpy of formation of pure compounds using molecular structure. *Aust. J. Chem.* **2009**, *62*, 376–381.

(45) Gharagheizi, F.; Tirandazi, B.; Barzin, R. Estimation of aniline point temperature of pure hydrocarbons: A quantitative structure−property relationship approach. *Ind. Eng. Chem. Res.* **2009**, *48*, 1678–1682.

(46) Gharagheizi, F.; Mehrpooya, M. Prediction of some important physical properties of sulfur compounds using QSPR models. *Mol. Divers.* **2008**, *12*, 143–155.

(47) Sattari, M.; Gharagheizi, F. Prediction of molecular diffusivity of pure components into air: a QSPR approach. *Chemosphere* **2008**, *72*, 1298–1302.

(48) Gharagheizi, F.; Alamdari, R. F.; Angaji, M. T. A new neural network−group contribution method for estimation of flash point. *Energy Fuels* **2008**, *22*, 1628–1635.

(49) Gharagheizi, F.; Fazeli, A. Prediction of watson characterization factor of hydrocarbon compounds from their molecular properties. *QSAR Comb. Sci.* **2008**, *27*, 758–767.

(50) Gharagheizi, F.; Alamdari, R. F. A molecular-based model for prediction of solubility of C_{60} fullerene in various solvents. *Fullerenes, Nanotubes, Carbon, Nanostruct.* **2008**, *16*, 40–57.

(51) Gharagheizi, F. A new neural network quantitative structure−property relationship for prediction of θ (lower critical solution temperature) of polymer solutions. *e-Polymers* **2007**, *114*, 001[2007].

(52) Gharagheizi, F. QSPR studies for solubility parameter by means of genetic algorithm-based multivariate linear regression and generalized regression neural network. *QSAR Comb. Sci.* **2008**, *27*, 165–170.

(53) Gharagheizi, F. A chemical structure-based model for estimation of upper flammability limit of pure compounds. *Energy Fuels* **2010**, *27*, 3867–3871.

(54) Mohammadi, A. H.; Martínez-López, J. F.; Richon, D. Determining phase diagrams of tetrahydrofuran+methane, carbon dioxide or nitrogen clathrate hydrates using an artificial neural network algorithm. *Chem. Eng. Sci.* **2010**, *65*, 6059–6063.

(55) Vatani, A.; Mehrpooya, M.; Gharagheizi, F. Prediction of standard enthalpy of formation by a QSPR Model. *Int. J. Mol. Sci.* **2007**, *8*, 407–432.

(56) Mehrpooya, M.; Gharagheizi, F. A molecular approach for prediction of sulfur compounds solubility parameters, phosphorus sulfur and silicon and related elements. *Phosphorus Sulfur* **2010**, *185*, 204–210.

(57) Mehrpooya, M.; Mohammadi, A. H.; Richon, D. Extension of an artificial neural network algorithm for estimating sulfur content of sour gases at elevated temperatures and pressures. *Ind. Eng. Chem. Res.* **2010**, *49*, 439–442.

(58) Kalogirou, S. A. Artificial Neural Networks in renewable energy systems applications: A review. *Renewable Sustainable Energy Rev.* **2001**, *5*, 373–401.

(59) Lydersen, A. L. Estimation of Critical Properties of Organic Compounds. Report 3, Engineering Experimental Station, College of Engineering, University of Wisconsin, Madison, WI, 1955. *Ind. Eng. Chem. Res.*

(60) Joback, K. K.; Reid, R. Estimation of pure component properties from group contribution. *Chem. Eng. Commun.* **1987**, *57*, 233–247.

(61) Smith, J. M.; Van Ness, H. C.; Abbott, M. M. *Introduction to Chemical Engineering Thermodynamics*, 6th ed.; McGraw-Hill: New York, 2001.

(62) Housaindokht, M. R.; Bozorgmehr, M. R. Calculation of solubility of methimazole, phenazopyridine and propranolol in supercritical carbon dioxide. *J. Supercrit. Fluids* **2008**, *43*, 390–397.

(63) Gharagheizi, F. QSPR Analysis for Intrinsic Viscosity of Polymer Solutions by means of GA-MLR and RBFNN. *Comput. Mater. Sci.* **2007**, *40*, 159–167.

(64) Barna, L.; Blanchard, J. M.; Rauzy, E.; Berro, C. Solubility of flouranthene, chrysene, and triphenylene in supercritical carbon dioxide. *J. Chem. Eng. Data* **1996**, *41*, 1466–1469.

(65) McHugh, M.; Paulaitis, M. E. Solid solubilities of naphthalene and biphenyl in supercritical carbon dioxide. *J. Chem. Eng. Data* **1980**, *25*, 326–329.

(66) Yun, S. L. J.; Liong, K. K.; Gurdev, S. G.; Foster, N. R. Solubility of cholesterol in supercritical carbon dioxide. *Ind. Eng. Chem. Res.* **1991**, *30*, 2476–82.

(67) Garmroodi, A.; Hassan, J.; Yamini, Y. Solubilities of the drugs benzocaine, metronidazole benzoate, naproxen in supercritical carbon dioxide. *J. Chem. Eng. Data* **2004**, *49*, 709–712.

(68) Weinstein, R. D.; Muske, K. R.; Moriarty, J.; Schmidt, E. K. The solubility of benzocaine, lidocaine, and procaine in liquid and supercritical carbon dioxide. *J. Chem. Eng. Data* **2004**, *49*, 547–552.

(69) Cheng, K. W.; Tang, M.; Chen, Y. P. Solubilities of benzoin, propyl 4-hydroxybenzoate and mandelic acid in supercritical carbon dioxide. *Fluid Phase Equilib.* **2002**, *201*, 79–96.

(70) Huang, Z.; Lu, W. D.; Kawi, S.; Chiew, Y. C. Solubility of aspirin in supercritical carbon dioxide with and without acetone. *J. Chem. Eng. Data* **2004**, *49*, 1323–1327.

(71) Yamini, Y.; Bahramifar, N. Solubility of polycyclic aromatic hydrocarbons in supercritical carbon dioxide. *J. Chem. Eng. Data* **2000**, *45*, 53–56.

(72) Miller, D. J.; Hawthorne, S. B.; Clifford, A. A.; Zhu, S. Solubility of polycyclic aromatic hydrocarbons in supercritical carbon dioxide from 313 to 523 K and pressures from 100 to 450 bar. *J. Chem. Eng. Data* **1996**, *41*, 779–786.

(73) Gregorowicz, J. Solubilities of lactic acid and 2-hydroxyhexanoic acid in supercritical CO_2. *Fluid Phase Equilib.* **1999**, *166*, 39–46.

(74) Karamer, A.; Thodos, G. Solubility of 1-octadecanol and stearic acid in supercritical carbon dioxide. *J. Chem. Eng. Data* **1988**, *34*, 184–187.

(75) lez, J. G. G.; Molina, M. J.; Rodríguez, F.; Mirada, F. Solubilities of phenol and pyrocatechol in supercritical carbon dioxide. *J. Chem. Eng. Data* **2001**, *46*, 918–921.

(76) Yan, J. S.; Tsai, F. N. Solubilities of 1-eicosanol and eicosanoic acid in supercritical carbon dioxide from 308.2 to 328.2 at pressures to 21.26 MPa. *J. Chem. Eng. Data* **1994**, *39*, 827–829.

Received for review July 19, 2010
Revised manuscript received September 25, 2010
Accepted September 27, 2010

IE101545G